Mass Flow Rate Scaling of the Continuum-Based Equations Using Information Preservation Method

Ehsan Roohi[1], Masoud Darbandi[2], Shidvash Vakilipour[3]
Sharif University of Technology, P. O. Box 11365-8639, Tehran, Iran

Gerry E. Schneider[4]
University of Waterloo, Waterloo, Ontario, N2L 3G1, Canada

Kinetic theory based numerical scheme such as direct simulation Monte Carlo (DSMC) and information preservation (IP) schemes properly solve micro-nano flow problems in transition and free molecular regimes. However, the high computational cost of these methods encourages the researchers toward extending the applicability of the continuum-based equations beyond the slip flow regime. In addition to correct velocity profile, the continuum-based equations should predict accurate mass flow rate magnitude. The second-order velocity slip models derived from the kinetic theory provide accurate velocity profiles up to Kn=0.5; however, they yield erroneous mass flow rate magnitudes because the basic Navier-Stokes equations are invalid for transition regime calculation. To remedy this shortcoming, the rarefaction effects must be considered on dynamic viscosity, i.e., $\mu=\mu(\text{Kn})$, in order to achieve correct mass flow rate magnitude despite using the kinetic-based slip model. Using shear stress distribution of IP simulations, we develop an analytical formula for dynamic viscosity for the early transition regime and use it to modify the continuum-based equations to improve more accurate mass flowrate magnitudes. Before using the IP results, we compare the accuracy of IP solution with the standard DSMC, the linearized Boltzmann and the continuum-based analytical solutions. Using the viscosity coefficient obtained from IP, the analytical expression for the mass flow rate is derived. We show that it provide accurate solutions for mass flow rate for the region of 0.1<Kn<0.5.

I. Introduction

The micro/nano geometries in MEMS-NEMS may work in a variety of flow regimes such as continuum, slip, and transition ones. The main characteristic to determine gas rarefaction is the Knudsen number; which is defined as the ratio of the mean free path of fluid to a characteristic dimension of the flow conduit (Kn=λ/H). For the flows with small Knudsen numbers, i.e., Kn<0.01, a continuum assumption is justifiable. In such flows, the analysis can be fulfilled via solving the Navier-Stokes (NS) equations. For flows with Knudsen numbers between 0.01 and 0.1, the non-equilibrium effects dominate in the flow near the wall surfaces, which can properly be described by applying new boundary conditions such as the velocity slip and temperature jump conditions to solve the NS equations. For flow with a Knudsen number greater than 0.1, high order kinetic effects become important and continuum-based analysis becomes less accurate. For Kn>10, the flow is in free molecular regime and intermolecular collisions are insignificant compared with the collisions between the gas molecules and their conducting walls [1,2]. For a typical flow in micro/nano geometries, Knudsen number varies due to pressure-temperature changes; therefore, mixed flow regimes such as slip-transition is usually observed. Basic Navier-Stokes equations with modification on their wall boundary conditions can be used to solve the flow field in slip flow regime. Alternatively, the molecular-based approaches such as direct simulation Monte Carlo (DSMC) [3] or information preservation (IP) method [4] are usually applied to solve rarefied flow field as Knudsen number exceeds beyond the slip flow condition. But the high computational costs of molecular-based approaches promote great interest in extending the range of continuum-based equations application beyond the slip flow regime.

---

[1] Graduate student, Department of Aerospace Engineering.

[2] Professor, Department of Aerospace Engineering.

[3] Research fellow, Department of Aerospace Engineering.

[4] Professor, Department of Mechanical and Mechatronics Engineering, AIAA Associate Fellow.

To extend the applicability of the NS equations, different second-order slip velocity boundary conditions have been suggested. They accurately predict either the velocity profile or the mass flow rate. A comprehensive review of slip boundary conditions can be found in Ref. [5]. One of the most accurate second-order slip Boundary conditions is the one which is derived from the kinetic theory. It is suggested as [5]

$$U_s - U_w = \frac{2-\sigma_v}{\sigma_v}[Kn\frac{\partial u}{\partial y} + \frac{Kn^2}{2}\frac{\partial^2 u}{\partial y^2}] \tag{1}$$

This slip boundary condition gives accurate wall slip value up to Kn<0.5; however, it is not accurate at all in predicting the mass flow rate. Alternatively, the second-order slip velocity profile given by Aubert and Colin [6] only yields accurate mass flow rate prediction within the early transition regime. It is given by

$$U_s - U_w = \frac{2-\sigma_v}{\sigma_v}[Kn\frac{\partial u}{\partial y} + \frac{9}{8}Kn^2\frac{\partial^2 u}{\partial y^2}] \tag{2}$$

Beskok and Karniadakis developed a unified velocity model for the entire Kn regime [7] as follows

$$U_s - U_w = \frac{2-\sigma_v}{\sigma_v}[\frac{Kn}{1-bKn}] \tag{3}$$

where b is an arbitrary constant determined from the DSMC simulation, i.e., $b= -1$. Contrary to Eq. (2), this model only predicts a good shape of the velocity profile and is erroneous for mass flowrate prediction. In fact, the kinetic effects manifesting near the walls create a non-equilibrium region, named Knudsen layer, which extends up to a few (1~2) mean free paths away from the wall [8]. This region is characterized by departures from linearity of the stress-strain relationship and cannot be captured by the Stokes assumption. Any assumed slip velocity profile matches the real velocity profile either at the wall (i.e., slip velocity, inside the Knudsen layer) or at the centerline (maximum velocity, outside the Knudsen layer). As will be shown in the next section, the slip boundary conditions given by Eq. (1) is accurate inside the Kn layer and predicts a correct slip value in the Knudsen layer and this has been considered in its derivation [5]. Meanwhile, it underpredicts the maximum velocity in the main flow. This is due to different characteristics of the inner (Kn layer) and outer (main flow) layers, and the fact that no single velocity profile can provide exact solution in both layers. Additionally, the failure of NS equations in transition regime makes it difficult to suggest a single formula capable of predicting both the velocity profile shape and the mass flow rate accurately. To remedy this problem, Karniadakis et al. [5] suggested that the viscosity coefficient must be modified in order to account the rarefaction effects. In fact, the NS equations are derived via the Stokes assumption, hence, they are invalid in predicting flow in the transition regime. Instead of modifying stress-strain relationships by considering additional terms, which results in more complicated equations, there is a simple idea to modify the dynamic viscosity as a function of Knudsen and use this modified value to calculate shear stress from the Stokes relation. To do so, it is crucial to find correct variation of the dynamic viscosity with Knudsen. Based on the simple analytical relations for dynamic viscosity at the two limits of flow regimes (continuum and free molecular), Karniadakis et al. [5] assumed a hybrid formula for viscosity, which is given by

$$\frac{\mu(Kn)}{\mu_0} = \left[\frac{1}{1+\alpha Kn}\right] \tag{4}$$

where α is a parameter, which should be adjusted properly based on the DSMC data in order to correctly predict the mass flow rate. In order to correctly predict the mass flow rate, the simple form of Eq. (4) is required to be complicated with variation of α, e.g. an inverse tangent function [5]. Alternatively, an averaged value for α can be suggested.

In the current study, we suggest an empirical relation for viscosity coefficient in early transition regime (0.1<Kn<0.5) based on our IP simulation. We normalize shear stress value obtained from IP solution with velocity gradient so that the variation of viscosity coefficient with Knudsen can be captured. The calculated viscosity coefficient is combined with the second-order kinetic slip velocity boundary conditions (Eq. (1)) to either derive analytical expression for mass flow rate or increase the range of applicability of an already-developed NS solver for the transition regime. The developed analytical expressions and the modified NS solver are extensively validated against available analytical and experimental data. We also investigate the range of validity of the developed expressions. Some key points should be addressed about the contribution of the current work. First, although the pervious study of Karniadakis et al. [5] derives an expression for the viscosity coefficient for the entire transition regime, it has a limitation with respect to α, which its exact value is unknown. Therefore, their suggested formula, I.e., Eq. (4) cannot be easily extended to arbitrary flow regimes without a priority information about α. Second, the developed viscosity model has a comprehensive form that follows correct physical behavior of the flow field. Although it is obtained from the IP numerical simulations, it is close to experimentally-confirmed viscosity model

derived from the Colin relation, see Ref. [6]. Additionally, combining it with the second-order kinetic boundary conditions, which is quite accurate in predicting the slip velocity in the transition regime, it provides exact prediction for the mass flowrate. Third, previous study [5] used the DSMC mass flow rate to extract an analytical relation for the viscosity. Therefore, their procedure needs tremendous independent numerical efforts in addition to the fact that the DSMC data are quite noisy. In this study, we use IP shear stress to formulate the variation of viscosity coefficient with the Knudsen number. This in turn reduces the computational costs and derive a more general expression for the mass flow rate.

Based on this, we suggest an analytical solution for the mass flow rate inside channels. It is accurate in the early transition regime. We restrict ourselves to 0.1<Kn<0.5, where the slip velocity boundary conditions (based on the kinetic theory) are valid for this range and no alternative formula can be found to be accurate for this region.

II. The Viscosity Model

A. The DSMC-IP Method

It is widely accepted that the DSMC method is one of the most accurate methods to model rarefied gas flows numerically. In fact, DSMC simulates particle behavior in a consistent manner as described by the Boltzmann equation. The Boltzmann equation is the general governing equation for dilute gas. Consequently, the results of DSMC provide accurate solutions to the Boltzmann equation as long as the numerical approximations such as cell size, time step, inlet/outlet boundary conditions, and the inter-molecular and molecular-wall collision models are realistic. Although DSMC is a successful approach for simulating subsonic microflows [9-11], the statistical inherent scattering in DSMC prevents its efficient application to microflow at very low speeds. To remedy this shortcoming, Fan and Shen [4] developed the information preservation scheme. They used the DSMC molecular velocities as well as the preserved information velocities to record the collection of enormous number of molecules, which a simulated DSMC particle can represent. The preserved macroscopic information is solved in a similar manner to that for the microscopic information in the DSMC method and is then modified to include the pressure force, which is the main driving force for low speed flows. In fact, the IP scheme directly implements the pressure gradients in the preserved velocity field while the conventional DSMC just implements the pressure at the inlet/outlet boundaries, which really need longer time to affect the entire flow field. Consequently, the IP scheme greatly reduces the computational time compared with the standard DSMC simulators [12-13]. Sun and Boyd [14] further extended the IP method to simulate general subsonic microflows. They presented proper models for temperature field and modified molecular collision model. More details on the IP method can be found in Refs. [14-16].

B. Mass Flow Rate Validation for IP

Before applying our IP code for viscosity calculation, we need validating it with the IP simulation of Shen [15]. Figure 1 shows the variation of normalized mass flowrate $(\dot{m}^* = \dot{m}/(\rho_m \sqrt{2RT} h/2))$, where ρ_m is the average of the inlet-outlet densities, with inlet Knudsen number for the current IP and that of Shen's IP and the DSMC simulations. The pressure ratio is PR=1.428 and working flow is nitrogen. Good agreement is observed. Since the IP prediction of mass flow rate agrees well with that of DSMC, we can rely on our IP solution as a reliable Boltzmann equation solver. It is necessary to remind that the collision model of IP is a crucial parameter, which remarkably affects the shear stress calculation. The preliminary IP collision model [12-13], which assumes the preserved information of particles is the same after collision, is not a precise predictor for the viscosity and thermal conductivity. Sun and Boyd [14] suggested a phenomenological model for the distribution of the information after collision using the collision deflection angle and the experimental data. In the next sections, we use both collision models, i.e., collision model 1 and collision model 2 and implement the effects of collision model on the velocity profile prediction.
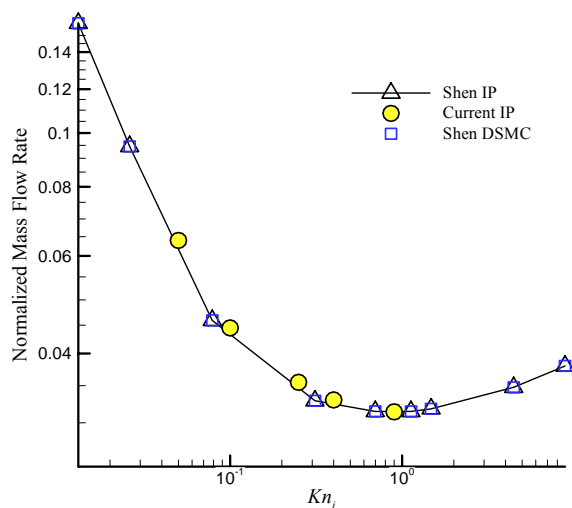
Figure 1. Mass flow rate variation with inlet Knudsen number, comparison between current IP simulation and results reported by Shen [15].

American Institute of Aeronautics and Astronautics

C. Shear Stress

We apply our scheme to calculate the dynamic viscosity variation with Knudsen number. The shear stress obtained from IP is used to obtain μ (Kn) as follows

$$\mu_{effective}(kn) = \frac{\tau_{w,IP}(x)}{\partial V_t / \partial n} \tag{5-a}$$

$$\tau_{w,IP} = \frac{\sum_{j=1}^{N_s} m(V_{t,j}^{in} - V_{t,j}^{re})}{t_s A} \tag{5-b}$$

where $\tau_{w,IP}$ is the IP shear stress calculated according to Eq. (5b), N_s is the total number of molecules striking the wall element during t_s, A is the area of the wall element, the subscript t denotes the tangential velocity component, n is the normal direction and the superscripts *in* and *re* denote the values before and after the wall element is hitted. For small Knudsen number flows, the linear dependence of stress-strain is kept; however, higher-order terms show up in the shear stress formula as Knudsen increases. We have

$$\tau_{w,IP} = \tau_w^{(NS)} + \tau_w^{(B)} + \tau_w^{(AB)} + ... = \mu_{NS}\frac{\partial V_t}{\partial n} + \tau_w^{(B)} + \tau_w^{(AB)} + O(Kn^4) \tag{6}$$

where superscripts NS, B, and AB stands for Navier-Stokes, Burnett and augmented Burnett equations, respectively. We therefore approximate Eq. (6) to obtain an effective viscosity coefficient for Navier-Stokes equations:

$$\tau_{w,IP}(x) \approx \mu_{effective,NS}(x)\frac{\partial V_t}{\partial n} + \tau_w^{(B)} + O(Kn^3) \approx \mu_{effective,NS}(x)\frac{\partial V_t}{\partial n} + O(Kn^3) \tag{7}$$

The value of $\tau_w^{(B)}$ is negligible for low Mach number isothermal flows in long channels [5]. Holding other stress terms in Eq. (6) (such as $\tau_w^{(AB)}$) is not useful for our current purpose in that the resulting viscosity coefficient must be applied to correct the mass flowrate of augmented Burnett equations not the NS equations. The validity of this approximation decreases for higher Knudsen number flows. In fact, the computed viscosity coefficient from Eq. (7) transforms the IP shear stress to the NS equations and permits these equations to be extended beyond the limit of slip flow regime while correctly predict the mass flowrate.

Figure 2 shows the variation of dynamic viscosity, which is normalized with the unmodified value at $Kn \rightarrow 0$, with Knudsen number in mid-transition regime and obtained from Eq. (7). The IP shear stress computed for a nitrogen flow in a channel with an aspect ratio (*L/H*) of 20 and a pressure ratio of 2. The full momentum accommodation is considered for the walls as $\sigma = 1$. Different independent runs were performed while the inlet Knudsen was increased to collect the required data. Figure 2 shows that dynamic viscosity rapidly falls in the early transition regime. It should be noted that the validity of Eq. (7) for higher Kn values is completely suspicious because the Knudsen layer (higher-order terms) grow and consequently a linear approximation turns to be invalid. Therefore, there is some error for viscosity as Knudsen approaches unity. In the current study, we concentrate on the limit of 0.1<Kn<0.5, where the slip prediction by Eq. (1) is accurate and there is little error in using Eq. (7).

Using Eq. (1) for the velocity slip, we do not include viscosity modification in the *y* direction, as suggested by Lockerby et al. [8]. They combined the viscosity coefficient with the wall-damping functions so that the nonlinear variation of the stress-strain in the Knudsen layer is correctly simulated. This strategy is usually employed with the slip velocity boundary conditions such as the first-order relations (which are inherently incorrect in slip prediction at higher Knudsen regimes) to correctly predict the velocity profile inside and outside the Knudsen layer. Since the concept of Knudsen layer is considered in the derivation of slip equation, see Eq. (1), this relation accurately predicts the slip value and the maximum
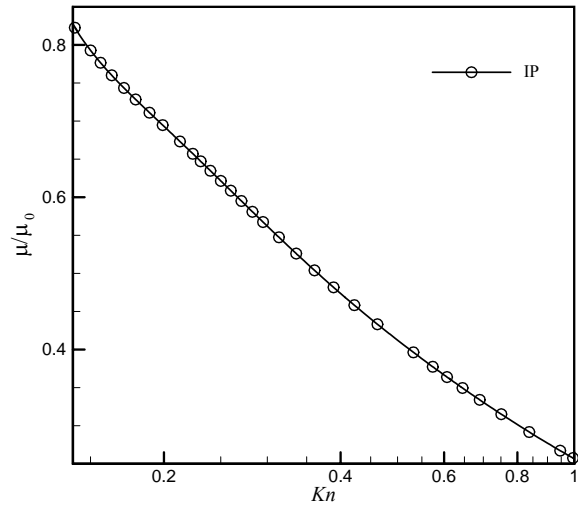
Figure 2. Variation of viscosity coefficient with *Kn* in mid-transition regime from IP solution.

American Institute of Aeronautics and Astronautics

velocity for a suitable range of Knudsen numbers. In other words, the slip boundary condition given by Eq. (1) is not a fictitious macro slip boundary condition, see Ref. [8], which over-predicts the slip value to capture the maximum velocity value correctly. As we show in the next sections, suggesting viscosity as a function of $Kn(x)$ is a suitable approach to predict the mass flow rate accurately while the original boundary condition, Eq. (1), predicts the slip and maximum velocities correctly. It should be reminded that a large scatter in DSMC data for the shear stress prevents its efficient application to viscosity calculation.

D. Viscosity Prediction via Experimental and IP Data

Analytical kinetic theories show that the viscosity coefficient becomes a function of Knudsen in transition regime. Kardianakis et al. [5] assumed a simple formula for the viscosity variation, see Eq. (4), and adjusted it via including a free parameter, which is determined using DSMC. This parameter is modified in such a way that the DSMC and NS mass flow rates match properly. Here, we suggest a more comprehensive approach to obtain an analytical formula for the viscosity coefficient. The first approach is to correlate the correct slip boundary condition formula with a correct mass flow rate relation as is described below.

Using the second-order slip boundary condition given by Eq. (1), the velocity profile of the flow field can be obtained from

$$u(x,y) = \frac{h^2}{2\mu} \frac{dp}{dx} [(\frac{y}{h})^2 - (\frac{y}{h}) - (\frac{2-\sigma}{\sigma})(Kn - Kn^2)] \tag{8}$$

For a general velocity slip boundary condition on the wall, the mass flow rate is obtained from

$$\dot{m} = \int_0^h (\rho u) dy = \int_0^h \frac{h^2}{2\mu RT} p dp \Phi(y, Kn) dy \tag{9}$$

where density is substituted from the equation of state, $\rho = p/(RT)$, and Φ is a general relation obtained from the slip condition. Assuming an isothermal flow and considering that the pressure varies only in the axial direction, the only term remaining inside the integral is Φ. Integration along the axial direction would eventually yield the total mass flow rate as follows

$$\int_0^L \dot{m} dx = \dot{m}L = \int_{Pin}^{Pout} (\frac{h^2}{2\mu RT} \int_0^h \Phi(y, Kn) dy) p dp \tag{10}$$

We consider the viscosity coefficient as a function of Knudsen number, $\mu = \mu(Kn)$ and holds it inside the integral. Knudsen number is related to pressure via $Kn_o p_o = kn(x)p$, where the subscript o stands as the outlet. As stated in the last section, the second-order velocity profile given by Eq. (2), is named Colin model. It predicts an accurate mass flow rate. The mass flow rate corresponding to Eq. (2) is derived from

$$\dot{m} = \frac{h^3 p_o^2}{24\mu_0 RTL} (\Pi^2 - 1 + 12(\frac{2-\sigma_v}{\sigma_v})(\Pi - 1)Kn_o + 27Kn_o^2 \ln(\Pi)) \tag{11}$$

where Π stands for the pressure ratio (p_{in}/p_{out}). If we substitute Eq. (11) in the left hand side of Eq. (10) and keep the viscosity as a function of Knudsen, we obtain

$$\frac{h p_o^2}{12\mu_0} (\Pi^2 - 1 + 12(\frac{2-\sigma_v}{\sigma_v})(\Pi - 1)Kn_o + 27Kn_o^2 \ln(\Pi)) =$$
$$\int_{Pin}^{Pout} (\frac{1}{\mu(Kn)} \int_0^h [(\frac{y}{h}) - (\frac{y}{h})^2 + (\frac{2-\sigma}{\sigma})(Kn - Kn^2)] dy) p dp \tag{12}$$

Integration Eq. (12), we can obtain an expression for the viscosity coefficient as follows

$$(\frac{\mu(Kn)}{\mu_o})_{Colin} = \frac{\frac{\sigma}{2-\sigma} + 6Kn - 6Kn^2}{\frac{\sigma}{2-\sigma} + 6Kn + 13.5Kn^2} \tag{13}$$

As will be shown in the next section, this relation is accurate for the range Kn<0.3 in that the analytical expression of Colin agrees well with the experimental data until this point, see Fig. 6. Equation (13) suggests that the viscosity varies as the second-order fractional function of Knudsen number. Having this in mind, we similarly correlate the IP viscosity, predicted and shown in Fig. 2, for a range of 0.1<Kn<0.5. The suitable expression is suggested as

$$(\frac{\mu(kn)}{\mu_0})_{IP} = \frac{1 + 0.89kn + 4.70kn^2}{1 + 0.75kn + 19.98kn^2} \tag{14}$$

Figure 3 shows the dynamic viscosity as a function of Knudsen from IP correlation (Eq. (14) is named our IP-model), analytical expressions obtained from the Colin model (Eq. (13)), and the Beskok model (Eq. (4)) with constant and variable parameter α. It should be noted that a value of $\overline{\alpha}$ =2.2 is suggested for the nitrogen flow having a pressure ratio of 2.2, and Kn_0=0.2 [5]. Using this value for lower Kn regimes would result in errors. Therefore, as will be shown in section 3-2, we equate the mass flow rate from IP-model with the Beskok formula to obtain exact values for parameter α. The line over variable α refers to such condition. Some key conclusions can be reached respecting Fig. 3. First, the analytical expression obtained from the Colin model matches with the IP-model as long as Knudsen is smaller than 0.3. As noted earlier, this is the range of validity of Colin model as well. Second, the Beskok model with a constant α coincides with the IP and Colin models close to Kn~0.2, the point where α=2.2 is reported. While we use variable α parameter, close agreement is observed for the region where Kn<0.25.
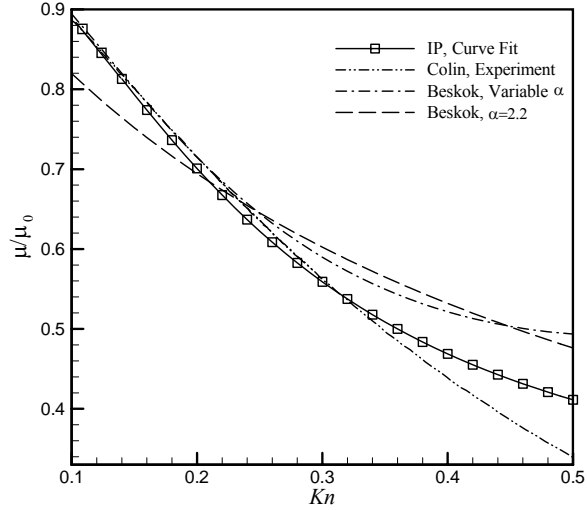
**Figure 3. Variation of viscosity coefficient with Kn from different methods, 0.1<Kn<0.5.**

Although IP-model is derived from the numerical simulation with specific conditions, i.e., a full momentum accommodation factor and Kn_{out}=0.2, we will show in the next sections that it does not restrict to these conditions and performs well over a wide range of accommodation coefficients and outlet Knudsen numbers.

Besides these conclusions, we remind that the viscosity coefficient by itself does not determine the mass flow rate but its combination with the slip boundary condition (this combination is called slip coefficient) determines the mass flow rate. For example, combining the Beskok viscosity formula with his unified velocity model (Eq.(3)) accurately predicts the mass flow rate for Kn>0.25. However, as was already mentioned, the kinetic-based second-order slip boundary condition is accurate for Kn<0.5 because the concept of Knudsen layer is respected in its derivation. This is while Eq. (3) depends on the arbitrary parameters obtained from the DSMC solution. Therefore, it can be accepted that the viscosity equations derived for this boundary condition are closer to actual physics of rarefied flows. This claim is supported with in accordance to the Colin model, which is in agreement with experimental data. Due to the importance of velocity profile, we will compare the velocity profiles from different slip conditions and then compare the mass flow rates derived from mixed velocity/viscosity models.

E. The Velocity Profiles

Figure 4 provides a comparison between different velocity profiles from the current DSMC-IP solution (with two collision models), Ohwada et al. linearized Boltzmann (LB) solution [17], Beskok analytical solution (Eq. (3)), and the developed numerical NS solver using the second-order kinetic slip velocity model (Eq. (1)) for different Knudsen numbers. The developed solver uses a finite-volume-based finite-element method [18-19]. More details on numerical scheme can be found in the cited references and not presented here because it is out of the main concern of this paper. The developed solver has extensively been validated with DSMC, Lattice Boltzmann solution and different experimental data and analytical solutions for micro/nano flows and heat transfer applications [20-24]. The velocity solutions obtained from this solver is the same as the analytical expression for the slip velocity given by Eq. (1). This figure gives valuable information about the accuracy of different numerical-analytical schemes. Following the discussion given in Sec. 2.A, the DSMC solution is considered as the closest solution to the Boltzmann equation. Therefore, we compare other solutions against that of DSMC. For the simulated cases, Ohwada Lattice Boltzmann solution greatly underpredicts the slip velocity comparing with the DSMC solution; however, it cprecisely follows the velocity profile curvature. The second-order kinetic model (Eq. (1)) is accurate for both the slip and maximum but it degrades as the Knudsen increases first for the maximum velocity, see Fig. (4c), and then for all the domain, see Fig. (4d), it is not shown for Kn=1.13. This is reasonable because this model is derived based on a maximum thickness of one mean free path for Knudsen layer, which is valid for a small Kn with a maximum of about Kn~0.5. The key point concluded from Fig. 4 is the slight inaccuracy of the IP solution for both the slip (overprediction) and maximum velocity (underprediction) for a flow with a Kn number less than 0.667. The last simulation with IP confirmed the fact that the IP velocity prediction is not coincident with that of DSMC [12]. Both IP collision schemes show this discrepancy while the second collision model performs slightly better. Meanwhile, as noted in

American Institute of Aeronautics and Astronautics

Sec. 2.B., IP predicts the mass flow rate closer to DSMC, which means that the errors in minimum/maximum points in velocity profile relatively compensate each other. As Knudsen increases, the Beskok analytical model (Eq. (3)) overpredicts the slip velocity (Fig. (4c)); however, it correctly predicts the maximum velocity. Our simulations show that the combination of our viscosity model (Eq. (14)) with the second-order kinetic model accurately predicts the mass flow rate for the mid-range transition regime (0.1<Kn<0.5) for different accommodation coefficients and the outlet Knudsen numbers as compared with the experimental data [25]. Since the second-order kinetic model is accurate within this Knudsen range, our viscosity model is physically accurate. This means that the IP errors in the velocity profiles do not reflect back in the viscosity coefficient calculation because IP provides correct mass flow rate magnitude.
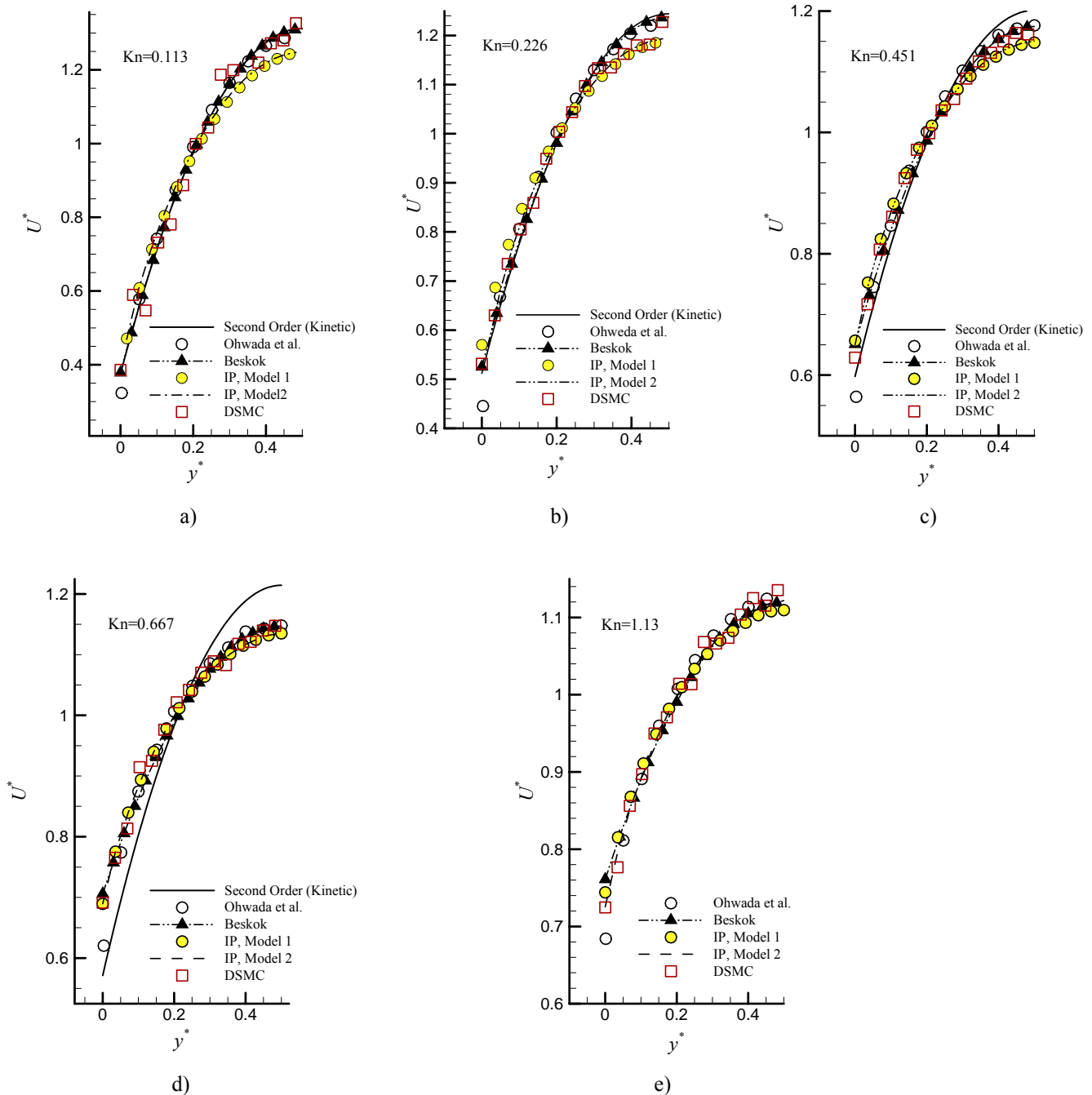
Figure 4: Comparison of velocity profile from different molecular and continuum based models at different Knudsen numbers.

Table 1: Coefficients for the normalized volumetric flow rate, Eq. (15).

	Model	C_1	C_2	$\mu(kn)/\mu_0$
1	First order (Maxwell)	$\dfrac{2-\sigma}{\sigma}$	0	1
2	Second order Kinetic (Beskok)	$\dfrac{2-\sigma}{\sigma}$	$-\dfrac{2-\sigma}{\sigma}$	$\dfrac{1}{1+\alpha Kn}$
3	Second order (Colin)	$\dfrac{2-\sigma}{\sigma}$	27/12	1
4	Hadjiconstantinou (Modified Cercignani model)	1.11	0.62	1

III. Mass Flow Rate Prediction

A. Analytical expression derivation

Obtaining the analytical expressions for the viscosity coefficient, i.e., Eqs. (13)-(14), we combine them with the velocity slip suggested in Eq. (1) to analytically calculate the mass flowrate. The normalized volumetric flowrate can be defines as

$$\frac{\dot{Q}}{\dot{Q}_c} = \frac{1}{\mu(kn)}[1+6(C_1 kn - C_2 kn^2)] \tag{15}$$

where the subscript c means the continuum regime and C_1 and C_2 are coefficients appearing behind Kn and Kn^2 terms in the velocity slip models. Table 1 gives values of C_1, C_2 and $\mu(kn)$ for some important slip models that we compare their accuracy with the current model. Using the second-order kinetic slip velocity and IP-based viscosity models, Eq. (15) can be rewritten as

$$\frac{\dot{Q}}{\dot{Q}_c} = \frac{1}{\mu(kn)}[1+6\frac{2-\sigma}{\sigma}(kn-kn^2)] = \frac{1+0.75kn+19.98kn^2}{1+0.89kn+4.70kn^2}[1+6\frac{2-\sigma}{\sigma}(kn-kn^2)] \tag{16}$$

Multiplying it by density, assuming $\sigma = 1$, and integrating along the axial direction, we can obtain an analytical expression for the normalized mass flow rate, i.e., slip coefficient, S, as follows

$$S = \frac{\dot{m}}{\dot{m}_c} = 1 + a_1 \frac{kn_o}{\Pi+1} + \frac{kn_o^2}{(1-\Pi^2)}(51.0\ln(\Pi)+34.07\ln(a_2))$$

$$a_1 = 11.72 + \frac{89.9\times 0.47}{1+(0.21+\frac{0.47}{kn_o})(0.21+\frac{0.47\Pi}{kn_o})}, \quad a_2 = \frac{1+0.89kn_o+4.7kn_o^2}{\Pi^2+0.89kn_o\Pi+4.7kn_o^2} \tag{17}$$

where Π is the pressure ratio. Note that the coefficients of Knudsen in the IP viscosity model reappear in the slip coefficient. For the general second-order boundary condition, the slip coefficient is given by

$$S = 1 + 12C_1\frac{Kn_o}{\Pi+1} + 12C_2\frac{Kn_o^2}{\Pi^2-1}\ln(\Pi) \tag{18}$$

Although Eq. (18) seems quite simple, it is derived from a velocity profile which is either correct for mass flow rate or the velocity profile prediction. It includes no viscosity correction. Collecting the both aspects together, it results in a comprehensive formula such as Eq. (17). Similarly, Karniadakis et al. [5] derived a relation for slip coefficient based on their unified velocity profile (Eq. (3)) and their empirical relation for viscosity coefficient (Eq. (4)), which yields

$$S = \frac{\dot{m}}{\dot{m}_c} = \frac{\Delta p}{(\Pi^2-1)p_o}(\Pi+1+2[6\frac{2-\sigma}{\sigma}+\overline{\alpha}]Kn_o + 12\frac{2-\sigma}{\sigma}\frac{b+\overline{\alpha}}{\Pi-1}Kn_o^2\ln(\frac{\Pi-bKn_o}{1-bKn_o})) \tag{19}$$

where $\Delta p = p_{in} - p_{out}$. As noted earlier, it is difficult to obtain variation of α for different Kn conditions. Therefore, an averaged value is suggested in Eq. (19). They reported a value of $\overline{\alpha} = 2.2$ for the nitrogen flow with $Kn_o=0.2$ and $L/h=20$. The main advantages of Eq. (17) over the Karniadakis et al. model is the fact that it does not depend on any arbitrary constant. Despite this fact, it suitably matches the experimental data for the entire range of Kn, which was derived previously.

B. Comparison of Different Slip Models

Developing analytical expressions for the volumetric and mass flow rates, we investigate the accuracy of new viscosity formula (the IP-model) against the analytical, numerical and experimental data. Figure 5 shows the volumetric flowrate obtained from different analytical expressions including the first-order slip boundary condition, the second-order slip boundary condition (the kinetic, Colin, and Hadjiconstantinou formula, see Table 1), the Beskok model, the current IP-model, and the numerical results from our NS solver using Eq. (14) to predict the dynamic viscosity. The kinetic-based second-order performs as the worst model. It is expected because it was derived only to predict a correct slip velocity. In fact, all models, which ignore the variation of viscosity coefficient with rarefaction yield poor prediction of mass flow rate. Meanwhile, the current IP-based model performs quite well. As will be shown later, the second-order model of Colin is accurate up to Kn<0.3. The results of our model agree with it up to this point and then approach to the results

Figure 5. Variation of volumetric flow rate with Knudsen number, comparisons of different analytical models and numerical NS solvers.

of Beskok formula. The Beskok formula performs far from the IP model for Kn<0.2 due to using an incorrect value for α. A constant value of 2.2 is used; however, this parameter changes abruptly for Kn<0.2. Interestingly, all the correct models have different curvatures, which are due to employing various slip-viscosity combinations. The numerical solution of the NS equations impose the current viscosity model and it shows good agreement with our IP-model.

Next we compare the derived mass flow rate values from different models. Figure 6 shows the variations of inverse slip coefficient (S^{-1} from Eqs. (17)-(19) with the constants taken from Table 1) with outlet Knudsen with a fixed pressure ratio PR=2. In addition to the preceding models, we also present the performance of Beskok slip model combined with the IP viscosity coefficient. Similar to Fig. 5, it is observed that the IP-model performs the closest one to the Colin data for Kn<0.3. After that, it approaches the Beskok model. The Beskok solution with a constant α overestimates the slip for K<0.3. Combination of the current IP model with the Beskok velocity slip provides a closer agreement with the Colin model; however, it does not match it exactly. In order to compare our results with the experimental data, the slip variation for PR=1.8 and $\sigma = 0.93$ was studied in this research and compared with the reliable experimental data of Colin [25]. According to Fig. 6b, the IP-model greatly follows the experimental data whereas the Colin formula departs from it as soon as Kn exceeds 0.3. The Beskok model does not match the experimental data at all for any Kn value. This may refer to the constant b used in Eq. (3), which was suggested as b=-1 for a full accommodation, or constant α [5]. This figure also shows low sensitivity of the IP viscosity coefficient to the accommodation coefficient. As was mentioned earlier, the IP simulations are performed for full momentum accommodation and currently applied for lower accommodation value. Figure 6c compares the slip coefficient variation with the average Knudsen ($Kn_m = (Kn_{in} + Kn_{out})/2$) from IP-model, Colin formula, Maurer et al. [26] experimental data, and their empirical formula given by

$$S = 1 + 6A_1 Kn_m + 12 A_2 Kn_m^2 \qquad (20)$$

For Nitrogen, A_1=1.3 and A_2=0.26. As is observed, the current model also agrees well with the experimental data of Maurer et al. [26] in the proposed range. We can conclude that the correct mass flow rate prediction of our IP and the suitable accuracy of the second-order kinetic boundary conditions can be considered as two important keys to achieve the current outcomes.

At this stage, we would like to find the correct variation of parameter α with Knudsen. Comparing the slip coefficients from our IP model with the Beskok formula performed on the test case shown in Fig. 6a, the variation of α can be calculated, see Fig. 7. As is observed, α starts from a value of 1.2, reaches to a peak around 2.35 at Kn=0.35, and then starts decreasing. For the range of our study, the average value is calculated to be $\bar{\alpha} = 2.07$, which is very close to the one reported in Ref. [5]. The behavior of Beskok viscosity model, while using a variable α was shown in Fig. 3. Using a variable α, the viscosity given by Eq. (4) shows a curvature similar to one by the IP-based viscosity; however, it is well-over it. The over-estimation of the viscosity is compensated with a higher
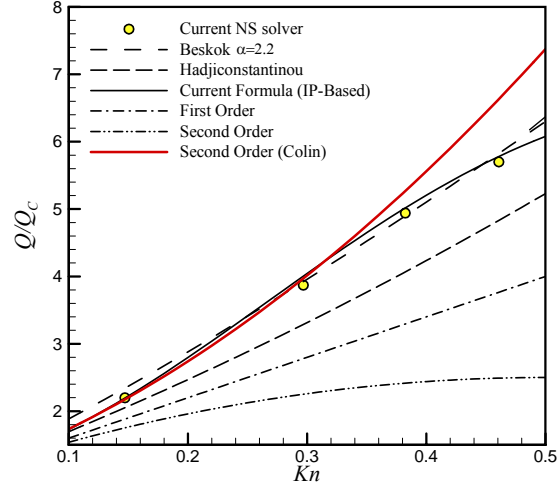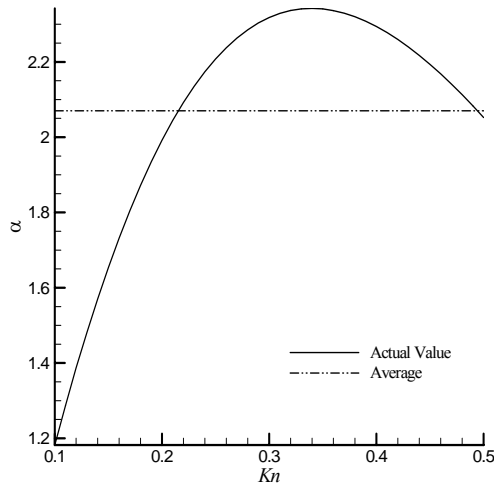
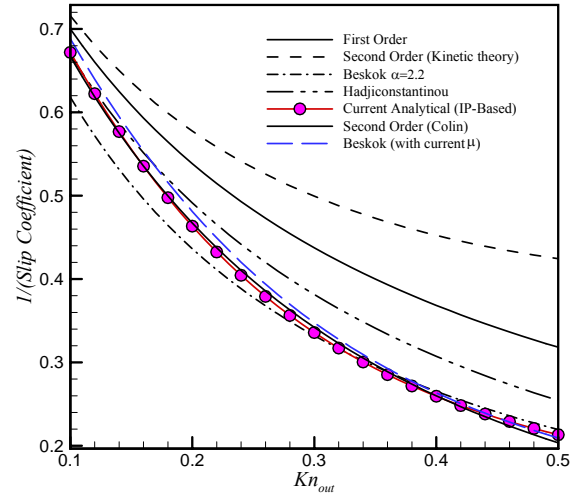value for the slip velocity predicted by the Beskok unified velocity formula, Eq. (3).

IV. Conclusion

To extend the basic NS equations beyond the slip flow regime calculation, we derived and validated an analytical expression for the variation of viscosity coefficient with Knudsen number using IP method. There are the second-order slip boundary conditions such as the kinetic-theory-based and the Beskok models, which accurately predict the velocity profile inside and outside of the Knudsen layer in high Knudsen number flows. To achieve correct mass flow rate in transition regime, it requires that the basic NS equations are modified to include the rarefaction effects properly. We modified the dynamic viscosity in a manner to let the NS equations capture the correct variation of the mass flow rate. In fact, the new viscosity model was obtained from the shear stress distribution provided by the IP simulations. Assuming a linear relation between the shear stress and the velocity gradient and limited accuracy of the kinetic-based slip model (up to $Kn<0.5$) did not permit us to extend the developed viscosity model to higher Knudsen values. Based on the new viscosity model, we developed analytical expressions for the mass flow rate. For the derivation range, $0.1<Kn<0.5$, the current IP-based model accurately predicted the mass flow rate. Comparing with previous models such as the Beskok model, a key advantage of the current model is that it does not depend on any unknown parameter, which can make the problem so complex.
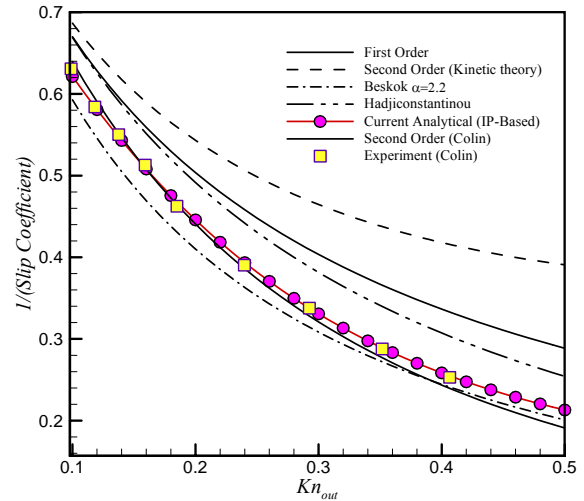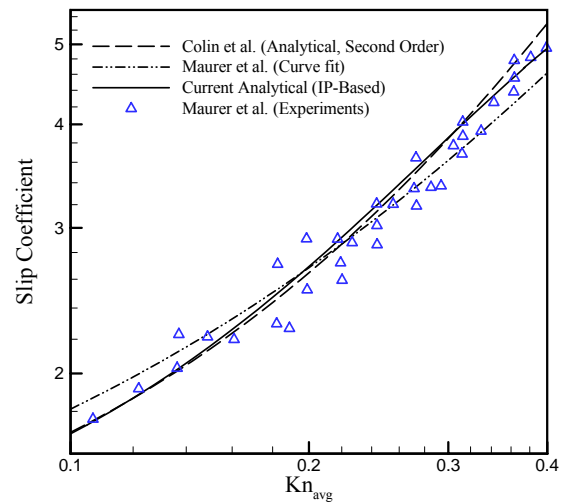

a) PR=2

b) PR=1.8, Sigma=0.93

c) PR=2

Figure 7: Parameter α (Eq. (4)) vs. Knudsen.

c) PR=2

Figure 6: Variation of inverse slip coefficient with the outlet Knudsen, comparison of different analytical models at two pressure ratios, experimental data [25, 26] are included.

10

References

[1] Ho, C., Tai, Y., Micro-electro-mechanical systems (MEMS) and fluid flows, Annual Review Fluid Mechanics, Vol. 30, 579–612, 1998.

[2] Kandlikar, S.G., Garimella, S., Li, D., Colin, S., King, M.R., Heat transfer and fluid flow in Minichannels and microchannels, Elsevier Ltd, U.K., 2006.

[3] Bird, G. A., Molecular Gas Dynamics and the Direct Simulation of Gas Flows, Clarendon, Oxford, 1994.

[4] Fan, J., Shen, C., Statistical simulation of low-speed unidirectional flows in transition regime, in: R. Brun et al. (eds.), Rarefied Gas Dynamics, Vol. 2, Cepadus-Editions, Toulouse, 1999.

[5] Karniadakis, G. E., Beskok, A., and Aluru, N., .Microflows and Nanoflows: Fundamentals and Simulation, Springer-Verlag, New York, 2005.

[6] Aubert, C. and Colin, S., High-order boundary conditions for gaseous flows in rectangular microchannels, Microscale Thermophys. Eng., 5(1), 41–54, 2001.

[7] Beskok, A., Karniadakis, G.E., A model for flows in channels, pipes, and ducts at micro and nano scales, Microscale Thermophys. Eng. 3, 43–77, 1999.

[8] Lockerby, D. A., Reese, J. M. & Gallis, M. A., Capturing the Knudsen layer in continuum-fluid models of nonequilibrium gas flows. AIAA J. 43, 1391, 2005.

[9] Fang, Y., Liou, W.W., Computations of the Flow and Heat Transfer in Microdevices Using DSMC with Implicit Boundary Conditions, Journal of Heat Transfer, 124 (2002) 338-345.

[10] Wang, M., and Li, Z., Simulations for gas flows in microgeometries using the Direct
Simulation Monte Carlo Method, International Journal of Heat and Fluid Flow, 25 (2004) 975–985.

[11] Roohi, E., Darbandi, M., Mirjalili, V., DSMC solution of supersonic scale to choked subsonic flow in micro to nano channels, ICNMM2008-62282, Proceedings of the 6th Int. ASME Conference on Nanochannels, Microchannels and Minichannels, Germany, 2008.

[12] Cai, C., Boyd, I. D., Fan, J., Candler, G. V., Direct simulation methods for low-speed microchannel flows, Journal of Thermophysics and Heat Transfer, 14(3), 368 2000.

[13] Fan, J., Boyd, I. D., Cai, C. P., Hennighausen, K., Candler, G. V., Computation of rarefied flows around a NACA 0012 airfoil, *AIAA J.* **39**(4), 618, 2001.

[14] Sun, Q., and Boyd, I.D., A direct simulation method for subsonic microscale gas flows, J. Computational Physics, 179 (2002) 400-425

[15] Shen, C., Rarefied Gas Dynamics; Fundamentals, Simulations and Micro Flows, Springer-Verlag Berlin Heidelberg, 2005.

[16] Liou, W. W., Fang, Y., Microfluid Mechanics; Principles and Modeling, McGraw-Hill, London, 2006.

[17] Ohwada T, Sone Y, Aoki K, Numerical analysis of the Poiseuille and thermal transpiration flows between two parallel plates on the basis of the Boltzmann equation for hard sphere molecules. Phys Fluids A 1:2042–2049, 1989.

[18] Darbandi M., and Vakilipour, S., Developing Implicit Pressure-Weighted Upwinding Scheme to Calculate Steady and Unsteady Flows on Unstructured Grids, International Journal for Numerical Methods in Fluids, Vol. 56 (2), pp. 115-141 2008.

[19] Darbandi M., and Vakilipour, S., Using Fully Implicit Conservative Statements to Close Open Boundaries Passing Through Recirculations., Int. Journal for Numerical Methods in Fluids, vol. 53, no. 3, pp. 371.389, 2008.

[20] Darbandi, M., and Vakilipour, S., Developing Consistent Inlet Boundary Conditions to Study the Entrance Zone in Microchannels., Journal of Thermophysics and Heat Transfer, 21(3) (2007) 596-607.

[21] Darbandi, M., and Vakilipour, S., A Compressible-Incompressible Algorithm to Study Dissipation Effect in Gaseous Microflows., Proceedings of the 15th Annual Conference of the CFD Society of Canada, Toronto, Ontario, Canada, 2007, pp. 1.8.

[22] Darbandi, M., and Vakilipour, S., Numerical study of flow and heat in long micro and nano channels, MNHT2008-52077, Proceeding of Micro/Nanoscale heat transfer international conference, Taiwan, 2008.

[23] Darbandi, M., and Vakilipour, S., Developing a consistent thermal boundary conditions at the inlet of microchannels, MNHT 2008-52131, Micro/Nanoscale heat transfer international conference, Taiwan, 2008.

[24] Vakilipour, S., and Darbandi, M., "Advancement in Numerical Study of Gas Flow and Heat Transfer in Microchannel," Journal of Thermophysics and Heat Transfer, Vol. 23, No. 1, pp. 205-208, 2009.

[25] Colin S, Rarefaction and compressibility effects on steady and transient gas flow in microchannels. Microfluid Nanofluidics 1(3):268–279, 2005.

[26] Maurer, J., Tabelin, P., Joseph, P. & Willaime, H., Second-order slip laws in microchannels for helium and nitrogen. Phys. Fluids 15, 2613–2621, 2003.